

# Preparation via gelling of porous $\text{Li}_2\text{ZrO}_3$ for fusion reactor blanket material

L. MONTANARO

*Department of Materials Science and Chemical Engineering, Politecnico, Torino, Italy.*

J. P. LECOMPTE

*Laboratoire Céramiques Nouvelles, Université, Limoges, France*

Crystalline powders of  $\text{Li}_2\text{ZrO}_3$  were prepared by gelling  $\text{ZrCl}_4$  and  $\text{CH}_3\text{COOLi}$  with  $\text{NH}_4\text{OH}$  at  $50^\circ\text{C}$ , at different pH values (5, 7 and 8) and for different times (3, 12 and 24 h), then drying and calcining. Compacts from these powders were found sinter to higher densities than a commercial  $\text{Li}_2\text{ZrO}_3$ ; their porosity at  $1200^\circ\text{C}$  was close to  $3\ \mu\text{m}$  and was suitable for blanket material applications. Tritium release as HTO begins at  $300^\circ\text{C}$  and reaches 73% at  $400^\circ\text{C}$ , a temperature much lower than that required for  $\text{Li}_2\text{O}$ .

## 1. Introduction

Current fusion reactor designs include a tritium breeding blanket for the production of tritium. To be considered as a candidate, material must (a) release tritium, (b) exhibit thermophysical, chemical and mechanical stability at high temperature, (c) be compatible with other blanket and structural materials, and (d) possess desirable irradiation behaviour.

In 1970, liquid lithium blanket designs dominated fusion reactor concepts, but since 1980 greater emphasis has been placed on the less chemically reactive ceramic lithium oxides such as  $\text{Li}_2\text{O}$ , lithium aluminate, silicate, zirconate and stannate. These compounds have a lithium atom fraction sufficiently high to produce adequate breeding ratios [1]. The materials properties are given in Table I, where  $T_m$  is the melting point,  $\rho_{\text{Li}}$  is lithium atom density,  $\rho_{\text{TD}}$  is bulk density and  $K$  is the thermal conductivity. The lower operating temperature limit is based upon estimates of tritium diffusion, and the upper temperature limit is based upon thermal sintering or restructuring effects.

A wide operating-temperature range, high lithium-atom density and thermal conductivity, low tritium solubility are all favourable properties. Finally, a solid ceramic breeder must have both a porous structure and a small grain size; porosity, pore morphology, and grain size have profound effects on thermal and mechanical properties, stability and tritium inventory. Impurities can affect thermodynamic and chemical properties as well as transport behaviour. Whereas substantial knowledge of the  $\text{Li}_2\text{O}$ ,  $\text{LiAlO}_2$ , and lithium silicates is now available, there is a lack of data on  $\text{Li}_2\text{ZrO}_3$ . This has a low tritium retention and exhibits excellent irradiation characteristics but little research has been dedicated to the synthesis of this compound.

Three polymorphic modifications of  $\text{Li}_2\text{ZrO}_3$  are reported in the literature but only two were encountered in this study. The polymorphic phase labelled " $\text{Li}_2\text{ZrO}_3$  I" is monoclinic and appears to be stable, its

melting point is above  $1500^\circ\text{C}$ . The polymorph " $\text{Li}_2\text{ZrO}_3$  II" is tetragonal: on heating for a long time or at high temperatures, conversion to  $\text{Li}_2\text{ZrO}_3$  I takes place:  $\text{Li}_2\text{ZrO}_3$  II appears to be metastable phase [3]. In this study, the preparation of  $\text{Li}_2\text{ZrO}_3$  powders via gelling was investigated in order to prepare powders sinterable at low temperature, giving a very uniform porosity in the sintered bodies.

## 2. Experimental procedure

To prepare lithium metazirconate, a solid state reaction of  $\text{Li}_2\text{CO}_3$  or  $\text{Li}_2\text{O}$  with  $\text{ZrO}_2$  was used [1,4]; however, in this process, the  $\text{ZrO}_2$  starting materials required extensive ball milling, introducing significant contamination from grinding media.

It was also proposed to use zirconium ethoxide [1] or zirconium propoxide with lithium ethoxide: nevertheless, this compound is not commercially available and must be prepared at the moment of the metazirconate synthesis. In this work, to simplify  $\text{Li}_2\text{ZrO}_3$  preparation, commercial products, such as zirconium propylate and lithium acetate, were used. This procedure does not provide the polymer chains necessary for reactants (Li, Zr, O) to attach themselves [5]; nevertheless, in a previous work [6], this method allowed preparation of  $\beta\text{-Al}_2\text{O}_3$  starting from aluminium isopropoxide and sodium acetate. For this reason the same technique has also been used for  $\text{Li}_2\text{ZrO}_3$  synthesis.

Lithium acetate (0.1 mol) was dissolved at  $25^\circ\text{C}$  in 1000 ml distilled and decarbonated water; then the zirconium propylate (0.05 mol) was added to the solution. The mixture was hydrolysed at  $50^\circ\text{C}$  under continuous stirring. To investigate the influence of the pH and of the hydrolysis time on the powders' characteristics, the reaction was carried out at pH 8, 7 and 5, controlled by acetic acid additions, and for 3, 12 and 24 h. One powder was also prepared by hydrolysing the precursors in ethanol for 3 h. Then the gels were

TABLE I Properties for candidate solid breeder materials [2].

Breeder	$T_m$ (K)	$\rho_{Li}$ (g cm <sup>-3</sup> )	$\rho_{TD}$ (g cm <sup>-3</sup> )	$K$ (W mK <sup>-1</sup> )	Operating temp. range (K)	Tritium solubility <sup>a</sup>
Li <sub>2</sub> O	1706	0.93	2.01	3.4	673–1073	L
LiAlO <sub>2</sub>	1883	0.27	2.61	2.2	723–1473	L
Li <sub>2</sub> SiO <sub>3</sub>	1473	0.36	2.53	1.5	683–1073	H
Li <sub>4</sub> SiO <sub>4</sub>	1523	0.54	2.35	1.5	583–1223	M
Li <sub>2</sub> ZrO <sub>3</sub>	1888	0.33	4.15	1.3	673–1673	M
Li <sub>8</sub> ZrO <sub>6</sub>	1568	0.68	2.99	1.5	623–1253	M

<sup>a</sup> L, low; M, moderate; H, high.

dried at 120 °C: the powders were amorphous and easy to mill.

The impurities in the powders calcined at 800 °C were detected by neutronic activation [7].

Thermal behaviour and structural change on dried powders were examined by differential scanning calorimetry (DSC), thermogravimetry (TG) (linear heating rate 10 °C min<sup>-1</sup>) and X-ray diffraction (XRD). Scanning electron microscopy was used to observe the morphology of the powders and sintered bodies. Grain sizes and surface areas were measured by laser granulometry and nitrogen adsorption (BET method). Dilatometric measurements (linear heating rate 10 °C min<sup>-1</sup>) were made on 3 mm × 3 mm × 25 mm bars, prepared by uniaxially pressing at 200 MPa.

On selected sintered pellets, the open porosity and the pore size distribution were evaluated by mercury porosimetry. On these sintered pellets the tritium emission was also evaluated, by Ente Nazionale Per Le Energie Alternative – Italian Nuclear Research Center (ENEA) [7].

### 3. Results and discussion

Table II shows the powder impurities detected by neutronic activation; it appears that the precursor hydrolysis in alcohol gives the purest powders, particularly as concerns the hafnium content. Therefore, this process allows the hafnium content to be reduced; the presence of hafnium affects nuclear reactions.

Laser granulometry gives an average particle size of 15 μm after 3 and 12 h hydrolysis; for longer hydrolysis times the average particle size becomes 20 μm. Longer hydrolysis times such as hydrolysis in alcohol, seem to favour agglomeration.

Typical DSC–TG curves are presented in Fig. 1. The endothermic peak below 100 °C and the related weight loss are due to evaporation of water. The exothermic peak at about 340 °C and the weight loss between 250 and 400 °C are related to organic compounds combustion and also to the loss of water. The endothermic peaks between 600 and 750 °C may be due to the reactions that give first Li<sub>2</sub>ZrO<sub>3</sub> II and then Li<sub>2</sub>ZrO<sub>3</sub> I, as supported by XRD analysis. A peak at about 1000 °C, that does not always appear in the DSC curves, may be ascribed to ZrO<sub>2</sub> traces [4]. The weight losses between 600 and 700 °C and between 900 and 1300 °C are due to OH<sup>-</sup> groups released during crystallization.

XRD patterns of as-prepared and calcined specimens are shown in Fig. 2. The powders dried at 250 °C

TABLE II Powder impurities by neutronic activation

Impurity	Powders obtained by hydrolysis in	
	water	alcohol
Hf	1.76 ± 0.05 wt %	1.45 ± 0.01 wt %
Sm	5.21 ± 0.07 p.p.m.	4.20 ± 0.3 p.p.m.
Lu	0.42 ± 0.01 p.p.m.	–
Br	2.10 ± 0.32 p.p.m.	5.27 ± 0.02 p.p.m.
Co	0.74 ± 0.2 p.p.m.	–
U	0.3 ± 0.06 p.p.m.	0.3 ± 0.06 p.p.m.

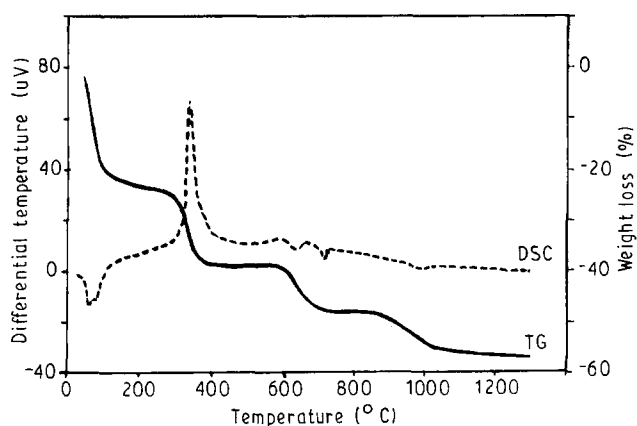


Figure 1 Typical DSC–TG curves of the prepared powders.

are still strongly amorphous. After heat treatment at 400 °C the presence of cubic ZrO<sub>2</sub> and Li<sub>2</sub>ZrO<sub>3</sub> is evident; Li<sub>2</sub>ZrO<sub>3</sub> is derived from carbonation of LiOH produced during the hydrolysis. Li<sub>2</sub>ZrO<sub>3</sub> formation, in the tetragonal phase, was first noted after calcining at 500 °C: its amount increases up to 700 °C. Starting from this temperature, ZrO<sub>2</sub> and Li<sub>2</sub>CO<sub>3</sub> are no longer detectable. The crystallization of Li<sub>2</sub>ZrO<sub>3</sub> I and Y phase begins at 700 °C. The Y phase, following the hypothesis of Enriquez *et al.* [3], may be a polymorph of lithium metazirconate or Li<sub>4</sub>ZrO<sub>4</sub> under stoichiometry in lithium. Starting from 800 °C, Li<sub>2</sub>ZrO<sub>3</sub> I increases and at 900 °C the powders contain only monoclinic Li<sub>2</sub>ZrO<sub>3</sub>.

All the samples lead to the same compound sequence: the influence of pH and hydrolysis time seems negligible. The powder obtained by hydrolysing the precursors in alcohol crystallizes less easily. This behaviour can be explained by considering that the precursor hydrolysis in alcohol is more difficult: the reaction between the hydroxides to give the metazirconate is less easy. A similar problem was found by

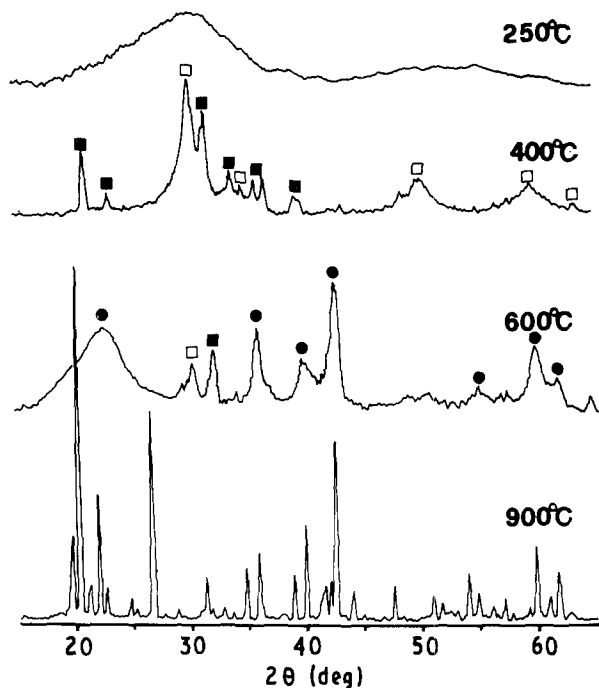


Figure 2 X-ray diffraction patterns of powders calcined at different temperatures. At 900 °C the powders contain pure  $\text{Li}_2\text{ZrO}_3$  I. (■)  $\text{Li}_2\text{CO}_3$ , (□)  $\text{ZrO}_2$ , (●)  $\text{Li}_2\text{ZrO}_3$  II.

Hirano *et al.* [8] during  $\text{LiAlO}_2$  synthesis. Scanning electron micrographs of powders, as-prepared and heat treated at 600 and 750 °C, are shown in Fig. 3. The amorphous zirconate agglomerates consisted of about 1  $\mu\text{m}$  particles that remained unchanged up to 600 °C. The size increased to 2–3  $\mu\text{m}$  or more on heating at 750 °C with  $\text{Li}_2\text{ZrO}_3$  II to  $\text{Li}_2\text{ZrO}_3$  I conversion.

The porosity of powder grains obtained by alcohol hydrolysis appears lower than that of the other powders. The adsorption isotherms of the powders dried at 120 °C are of type II: they are most frequently encountered when adsorption occurs on non-porous powders or on powders with pores larger than micropores [9] (Fig. 4).

The BET results show that the specific surface areas of the samples hydrolysed in water are, respectively, 35–40  $\text{m}^2 \text{g}^{-1}$  (pH = 5), 55–60  $\text{m}^2 \text{g}^{-1}$  (pH = 7), 50–60  $\text{m}^2 \text{g}^{-1}$  (pH = 8); the specific surface area of the sample hydrolysed in alcohol is 30  $\text{m}^2 \text{g}^{-1}$ . This last result confirms SEM observations, but it seems to be in opposition to Haberko's results on zirconia gel-derived powders [10]. This may be explained by supposing that the presence of lithium modifies the mechanism suggested, by Jones and Norman [11], to explain the reduction of the incidence of agglomerates in zirconia gel. In fact, from these works, the removal of non-bridging hydroxo-groups with alcohol leads to a reduction/elimination of hard agglomerates associated with the condensation reaction involving non-bridging hydroxo-groups.

The shrinkage at 1000 °C, measured on 3 mm  $\times$  3 mm  $\times$  25 mm pellets obtained from dried powders uniaxially pressed at 200 MPa, was 18–20% because of the volume change associated with the gel dehydroxylation reaction. Using powders treated at 700 °C, the shrinkage is much lower, particularly in

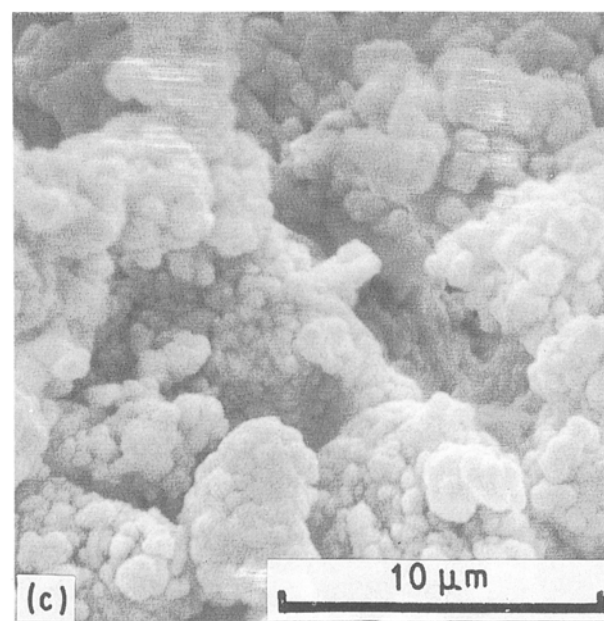
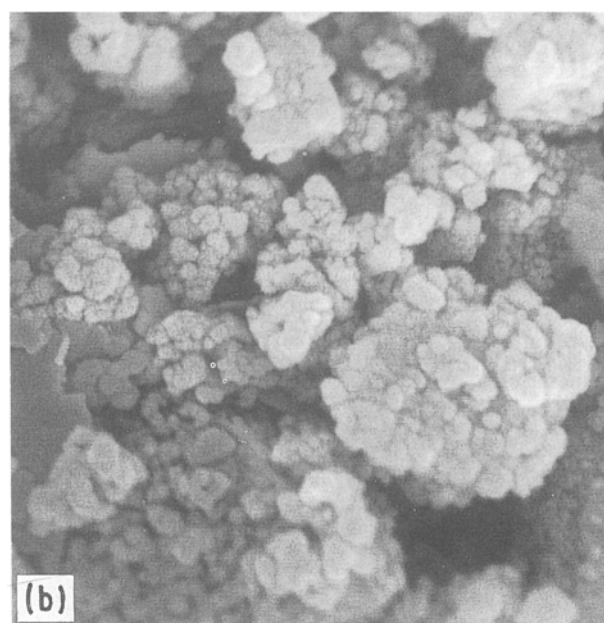
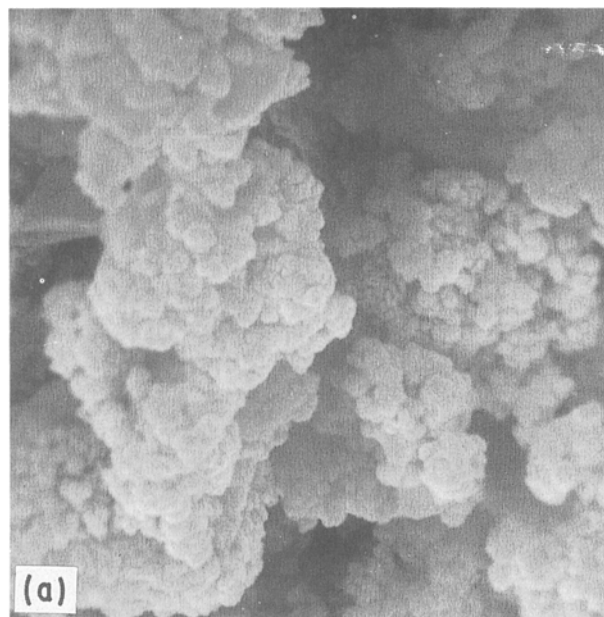


Figure 3 Scanning electron micrographs of powders: (a) as prepared; (b) heat treated at 600 °C; (c) heat treated at 750 °C.

the specimen made from powders obtained by hydrolysing the precursors in alcohol (Fig. 5); the lower shrinkage is related to the microstructure of the powder grains.

Pellets, made with the powders treated at 800 °C and pressed at 200 MPa, were sintered at 1000, 1100, 1200 and 1400 °C for 30 min. Fig. 6 shows scanning electron micrographs of the unpolished and fracture surfaces of sintered bodies. The microstructure of the samples treated at 1000 °C (Fig. 6a and b) can be described as dense regions having a size ranging from 5–15 µm, separated by interconnecting pores. Observations at 1100 °C were similar, except that the dense regions are larger (Fig. 6c and d). On reaching 1200 °C, most of the pores disappeared leaving dense, irregularly shaped agglomerates (Fig. 6e and f).

At 1300 °C the sintering is completed: on the surface no porosity was observed (Fig. 6g); on the fracture some small pores and a few fissures appeared (Fig. 6h). On the surface (Fig. 6i) and on the fracture (Fig. 6j) of the samples treated at 1400 °C, some large pores due to grain spheroidization were observed: the grain surface appears flaked.

Fig. 7 shows the pore size distribution for green and sintered bodies measured by mercury porosimetry. In the green body, the open porosity is about 32%, the pore radius ranges from 0.02–0.8 µm. It was observed in previous work [12, 13] that on increasing the sintering temperature the pore volume connected by the larger capillaries increases, whereas the pore volume connected by smaller capillaries decreases; at 1200 °C, the sintered bodies present a very uniform

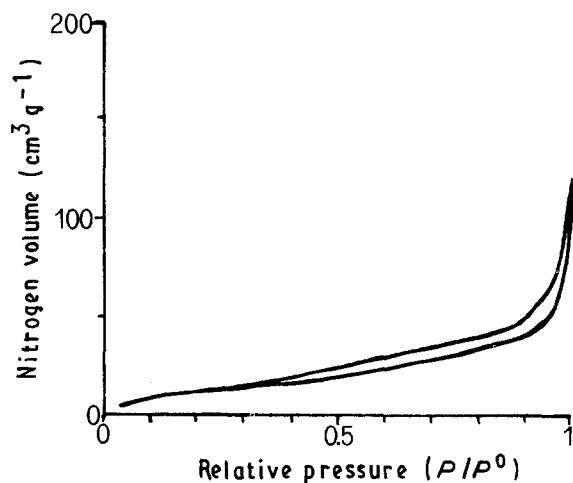


Figure 4 Typical nitrogen adsorption-desorption isotherms of the powders.

porosity centred at about 3 µm and about 85% of the pores sizes are close to this maximum.

At 1300 °C the mean open porosity is 12% and the pore volume redistributes to smaller capillaries: larger capillaries are very reduced.

At 1400 °C the mean open porosity increases to 16% and larger capillaries reappear: this phenomenon is the opposite of that observed during alumina [12] and alumina-zirconia [13] sintering.

From these results and from SEM observations it can be supposed that the phenomenon is due to lithium loss. Densities of the sintered bodies versus temperature are presented in Fig. 8 and compared with commercial material: fired densities are higher than that of the commercial material but still reach only 78% theoretical density of Li<sub>2</sub>ZrO<sub>3</sub> I [4].

On the bodies sintered at 1100 °C a thermal expansion coefficient of  $8.6 \times 10^{-6} \text{ °C}^{-1}$ , according to previous data [1, 4], was evaluated between 25 and 1200 °C; in this temperature range the expansion is reversible. Li<sub>2</sub>ZrO<sub>3</sub> samples sintered at 1200 °C were tested in the Create/ENEA circuit to evaluate tritium emission: this apparatus allows estimation of both the HTO and HT. The tritium release was obtained using a sweeping gas (He + 0.1% H<sub>2</sub>) having a 100 ml min<sup>-1</sup> flow and a temperature between 300 and 600 °C.

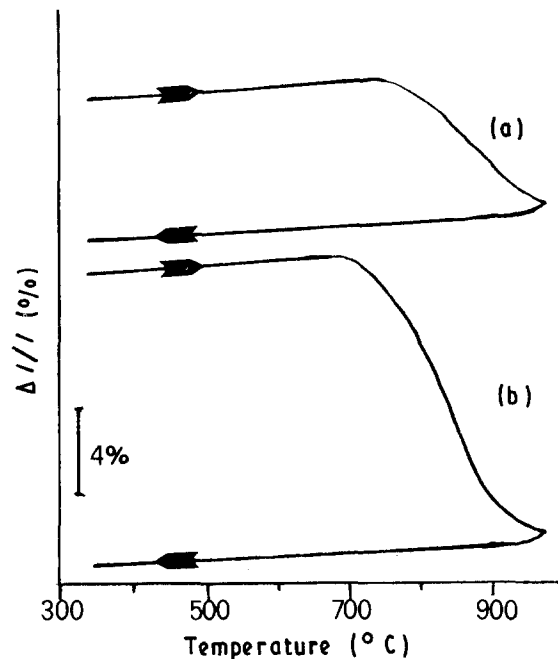


Figure 5 Dilatometric curves for powders obtained by hydrolysing the precursors: (a) in alcohol, (b) in water, and treated at 700 °C.

TABLE III Tritium release from sintered bodies of Li<sub>2</sub>ZrO<sub>3</sub>

Sample	Weight (g)	Density (g cm <sup>-3</sup> )	HT/T <sub>tot</sub> (%)	HTO/T <sub>tot</sub> (%)	Activity (mCi g <sup>-1</sup> )
1	0.0914	3.01	3.2	96.8	3.67
2	0.1168	3.01	9.1	90.9	2.60
3	0.1061	2.41	1.8	98.2	3.70

<sup>a</sup>T<sub>tot</sub> = total tritium release in the form of water-soluble (HTO) and water-insoluble (HT) components.

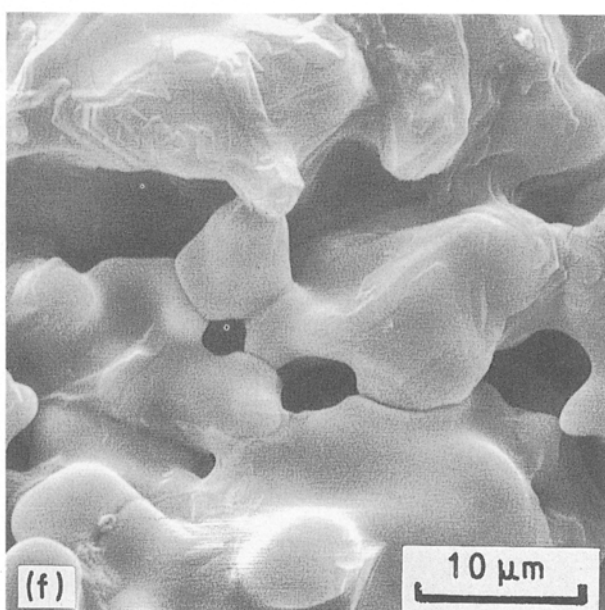
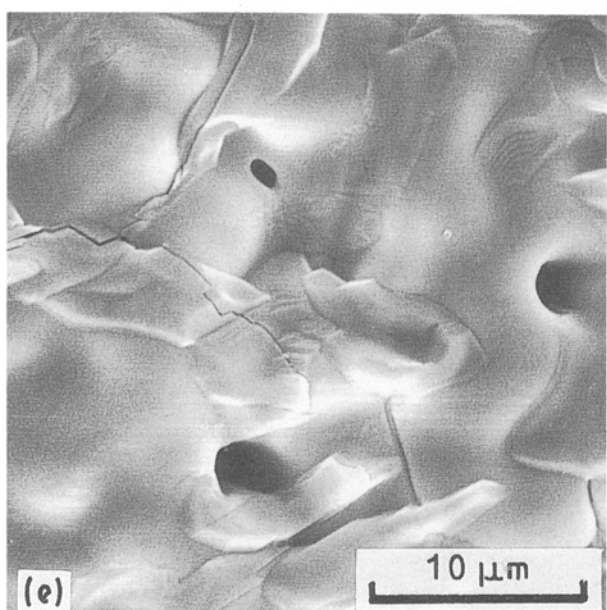
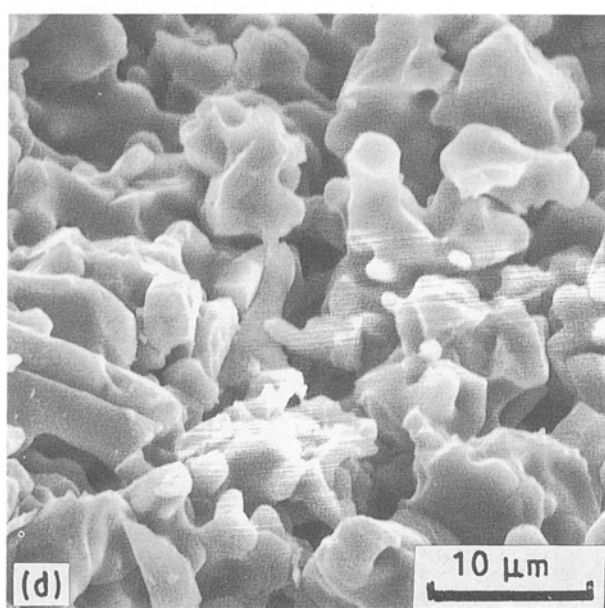
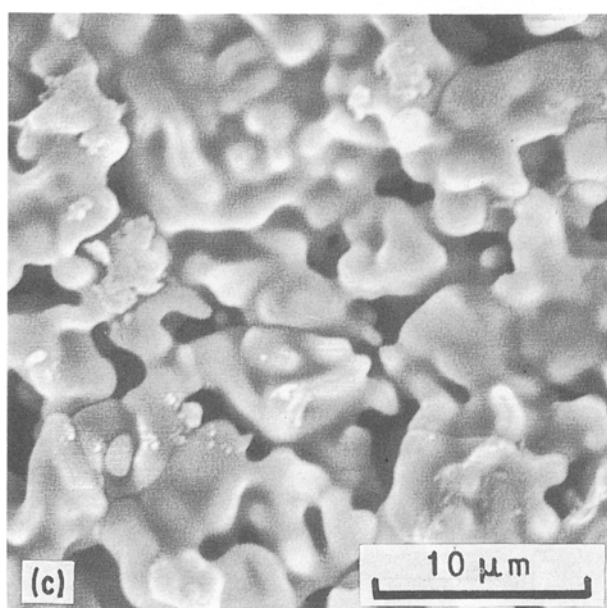
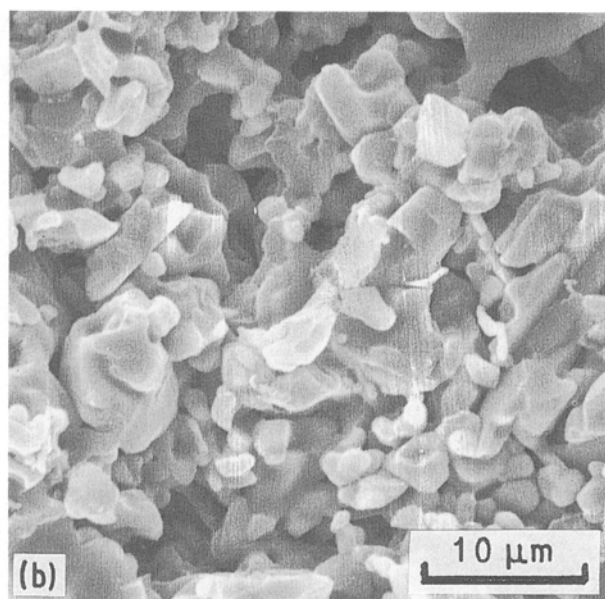
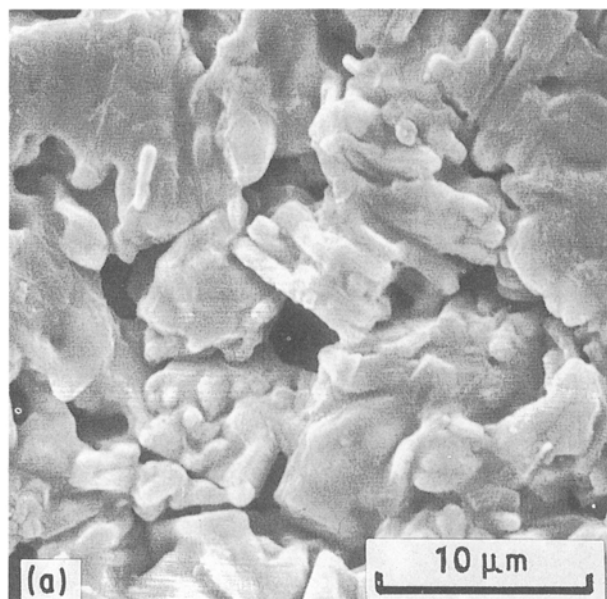


Figure 6 Scanning electron micrographs of (a, c, e, g, i) unpolished surfaces and (b, d, f, h, j) fracture surfaces of samples treated at: (a) 1000 °C, (b) 1000 °C, (c) 1100 °C, (d) 1100 °C, (e) 1200 °C, (f) 1200 °C, (g) 1300 °C, (h) 1300 °C, (i) 1400 °C, and (j) 1400 °C.

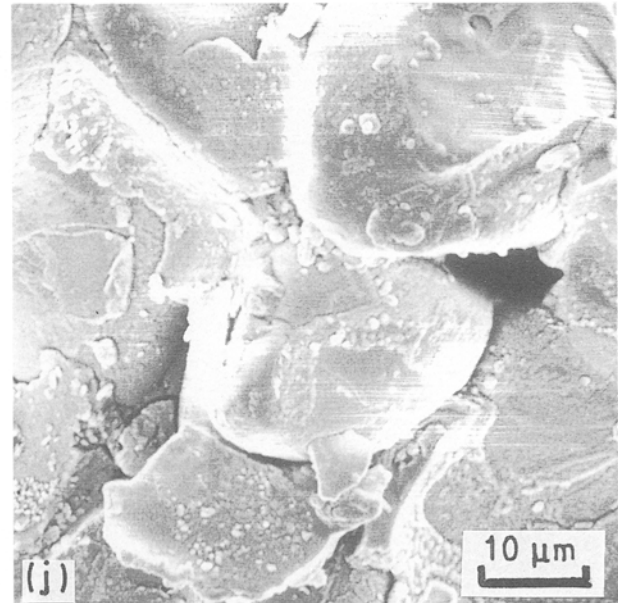
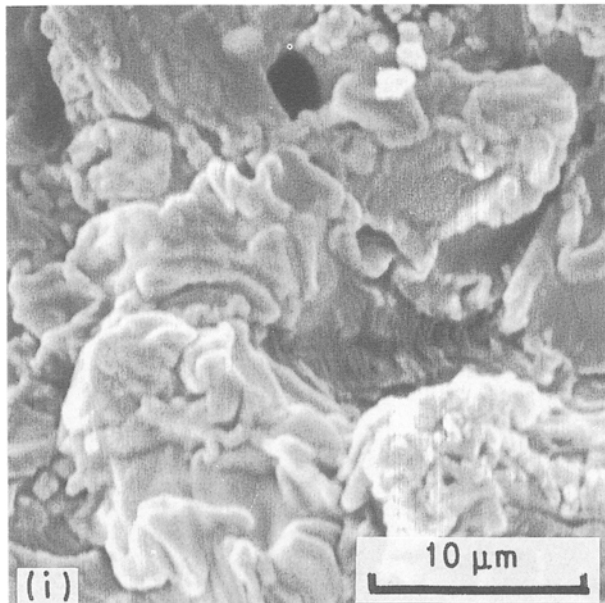
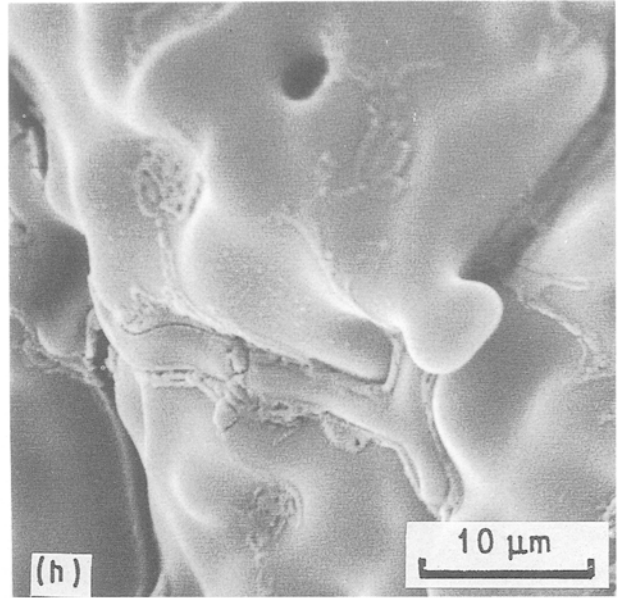
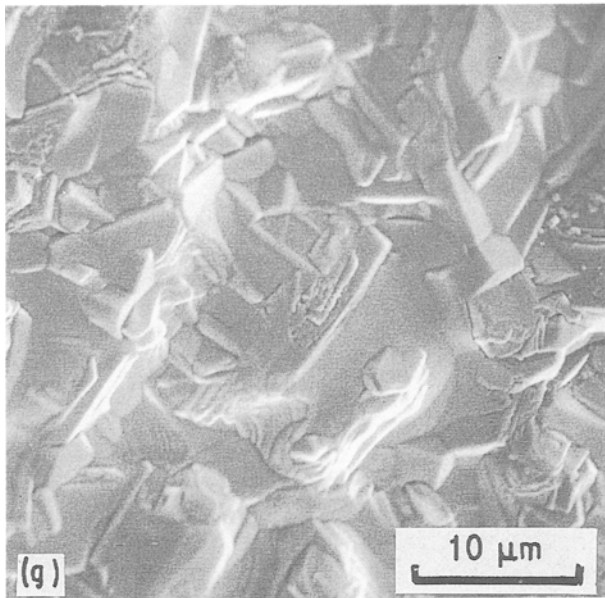


Figure 6 Continued.

Table III shows HT and HTO release from sintered bodies and tritium activity. From these results it appears that about 95% tritium is released as HTO.

As shown in Fig. 9, the lithium zirconate releases 33% drawn out tritium, beginning from 300°C and 73% at 400°C, temperature lower than with  $\text{Li}_2\text{O}$ . These results are comparable with those obtained by Inagaki *et al.* [14] for  $\text{Li}_2\text{SnO}_3$  and are reasonably explained as due to the small size of primary particles of  $\text{Li}_2\text{ZrO}_3$  and to the high porosity of the sintered bodies.

#### 4. Conclusions

1. As expected, the process proposed does not provide polymer chains: in fact  $\text{Li}_2\text{CO}_3$  and  $\text{ZrO}_2$  were identified at low temperature by XRD.

2. The time and the pH of the hydrolysis seem to have a negligible influence on the sintering behaviour and on the grain and pore sizes. The hydrolysis of the precursors in alcohol allows a purer, but more agglomerated powder to be obtained.

3. However, in all cases, it is possible to obtain pure  $\text{Li}_2\text{ZrO}_3$  at relatively low temperature and after short heat treatment times (30 min.).

4. The sintered bodies present a density higher than that of commercial materials, but still only 78% theoretical value. Heat treatment over 1300°C seems to give lithium loss.

5. The average tritium release as HTO is about 95%; 73% is already released at 400°C. This result is reasonably explained as being due to the small size of the primary particle of the zirconate and to the porosity of the sintered bodies.

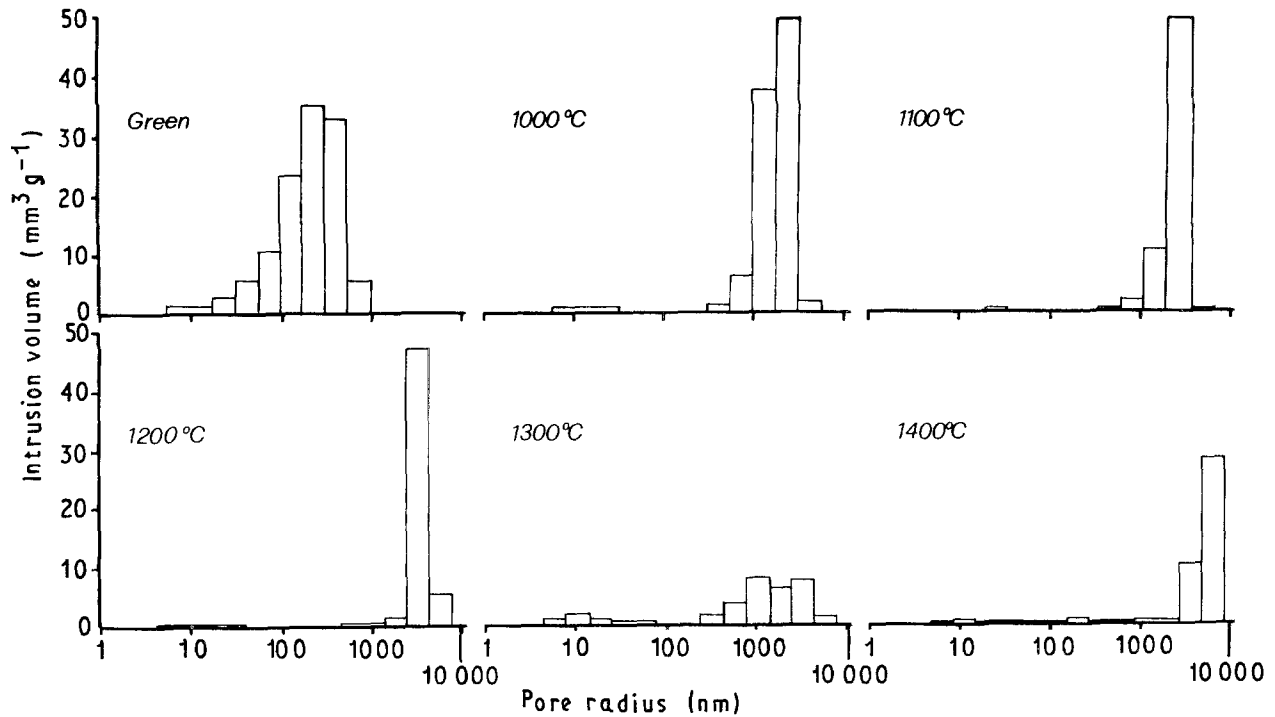


Figure 7 Pore size distribution in green and sintered bodies at different temperatures, evaluated by mercury porosimetry.

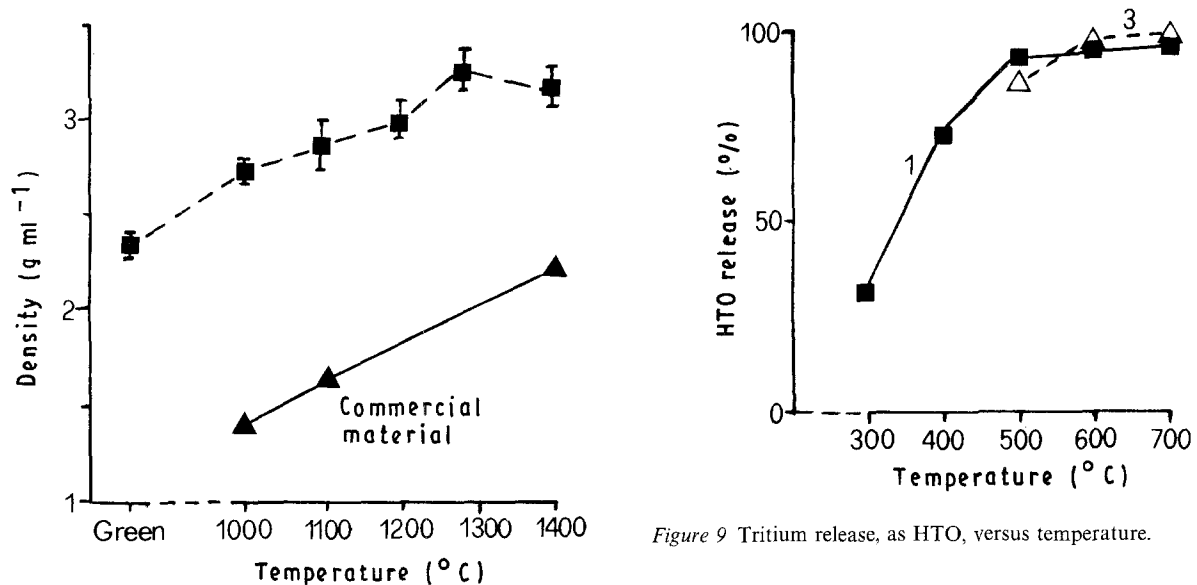


Figure 8 Density of sintered bodies versus temperature.

Figure 9 Tritium release, as HTO, versus temperature.

## References

- D. J. SUITER, J. W. DAVIS and B. A. KIRKPATRIK, *J. Nucl. Mater.* **103-104** (1981) 579.
- C. E. JOHNSON, K. R. KUMMERES and E. ROTH, *ibid.* **155-157** (1988) 188.
- L. J. ENRIQUEZ, P. QUINTANA and A. R. WEST, *Trans. Brit. Ceram. Soc.* **88** (1982) 17.
- C. ALVANI, L. BRUZZI, S. CASADIO, A. TUCCI and E. TOSCANO, *J. Europ. Ceram. Soc.* **5** (1989) 2195.
- J. P. BOILOT, F. CHAPUT and J. C. PAUXVIEL, *Silic. Ind.* **11-12** (1989) 187.
- G. COLUCCI, A. NEGRO, E. VISCONTE, C. PIJOLAT and R. LALAUZE, *Ceram. Int.* **16** (1990) 225.
- S. CASADIO, ENEA, private communication (1990).
- S. HIRANO, T. HAYASHI and T. KAGYAMA, *J. Amer. Ceram. Soc.* **70** (1987) 171.
- S. LOWELL and J. E. SHIELD, in "Powder surface area and porosity" (Chapman and Hall, London, 1984) p. 12.
- K. HABERKO, *Ceram. Int.* **5** (1979) 148.
- S. L. JONES and C. J. NORMAN, *J. Amer. Ceram. Soc.* **71** (1988) C190.
- F. F. LANGE, *ibid.* **67** (1984) 83.
- L. MONTANARO and A. NEGRO, *J. Mater. Sci.* **26** (1991) 4511.
- M. INAGAKI, S. NAKAI, T. TERAJ and Y. TAKAHASHI, *J. Ceram. Soc. Jpn* **98** (1990) 469.

Received 15 March  
and accepted 1 July 1991